High-resolution four-wave light-mixing studies of collision-induced coherence in Na vapor

L. J. Rothberg* and N. Bloembergen
Division of Applied Sciences, Harvard University, Cambridge, Massachusetts 02138
(Received 19 December 1983)

Near-resonant four-wave light mixing in Na vapor with inert buffer gases reveals collision-induced coherences when the difference frequency between two incident light beams equals the hyperfine splitting or the Zeeman splitting between two states of the $3\,^2S$ ground-state manifold. The Doppler broadening of the corresponding resonances decreases with increasing buffer-gas pressure. The width of the resonances becomes significantly narrower than the spontaneous linewidth of the near-resonant intermediate state and is determined by spin-exchange collisions between ground-state atoms. The dependence of the intensity of these collision-induced resonances on buffer-gas pressure and detuning from one-photon resonances is measured. Selection rules for various polarizations of the incident light fields and directions of an externally applied magnetic field are established.

I. HISTORICAL BACKGROUND

Early in the development of nonlinear optics it was explicitly noted that the calculation of complex nonlinear susceptibilities based on the evolution of the density matrix with damping terms yielded resonant terms with energy separations between pairs of initially unoccupied excited levels. Such terms do not occur in perturbation theories without damping.[1]

In the mid-1970s detailed studies of four-wave light mixing, including resonant Raman-Stokes and anti-Stokes scattering, required detailed expressions[2–4] for the nonlinear susceptibility $\chi^{(3)}$. Questions had been raised about its correct form, and occasionally procedures were used, where damping was added in an *ad hoc* fashion to results of perturbation theory without damping.[5–7] It was therefore important to cast general expressions for $\chi^{(2)}$ and $\chi^{(3)}$ in such a form that the terms with resonances between pairs of excited states are explicitly displayed.[2] Such terms, which have numerators proportional to an algebraic sum of damping parameters, are irretrievably lost if one starts with a perturbation approach without damping. The existence of these extra resonances was subsequently verified experimentally by Prior *et al.*,[8] firmly establishing the correct general complex form of $\chi^{(3)}$ in near-resonant situations.

Several authors have used double-sided Feynman diagrams[4,9–11] to facilitate the bookkeeping of the 48 terms in $\chi^{(3)}$. In the absence of damping, the $\langle$bra| and |ket$\rangle$ states evolve independently. In this case their relative time ordering is unimportant and single-sided diagrams could be used. To obtain the extra resonances the use of double-sided diagrams is necessary.

The essential aspects of the damping-induced extra resonances can be illustrated by a very simple calculation for a three-level system,[11] shown in Fig. 1(a). The system is initially in the ground state $\rho_{gg}^{(0)}=1$. Electric dipole matrix elements μ_{ng} and $\mu_{n'g'}$, connecting the ground state with two excited states, exist. The system is excited by two coherent fields at frequencies ω_1 and ω_2, respectively. The frequency ω_1 is near the resonant frequency ω_{ng}, and the frequency ω_2 is near the resonant frequency $\omega_{n'g'}$, so that

$$|\omega_1-\omega_2| \gg |\omega_1-\omega_{ng}| \approx |\omega_2-\omega_{n'g'}| \gg \Gamma_{ng} \approx \Gamma_{n'g} .$$

The dominant terms in the first-order solution are the induced coherences

$$\rho_{gn}^{(1)}(-\omega_1)=\frac{-\hbar^{-1}\mu_{gn}}{\omega_{gn}+\omega_1-i\Gamma_{gn}}E_1^* \tag{1a}$$

and

$$\rho_{n'g}^{(1)}(\omega_2)=\frac{\hbar^{-1}\mu_{n'g}}{\omega_{n'g}-\omega_2-i\Gamma_{n'g}}E_2 . \tag{1b}$$

In the second approximation one obtains the coherence at the difference frequency $\omega_2-\omega_1$,

$$\rho_{n'n}^{(2)}=\frac{-\hbar^2\mu_{gn}\mu_{n'g}}{(\omega_{n'g}-\omega_2-i\Gamma_{n'g})(-\omega_{ng}+\omega_1-i\Gamma_{ng})}E_2E_1^* \times\left[1-\frac{\Gamma_{ng}+\Gamma_{n'g}-\Gamma_{n'n}}{\omega_{n'n}-(\omega_2-\omega_1)-i\Gamma_{n'n}}\right] . \tag{2}$$

There are two contributions to this coherence depending on the time ordering of the perturbations at ω_1 and ω_2, respectively. The term with the resonant denominator $\omega_{n'n}-(\omega_2-\omega_1)-i\Gamma_{n'n}$ exactly cancels in the absence of

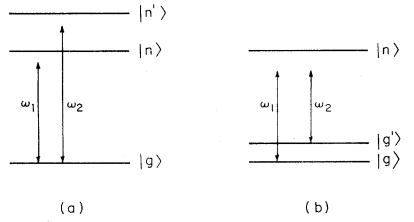

FIG. 1. (a) Collision-induced coherence $\rho_{n'n}^{(2)}(\omega_2-\omega_1)$ between two excited states, when initially only the ground state is occupied, $\rho_{gg}^{(0)}=1$. (b) Collision-induced coherence $\rho_{g'g}^{(2)}(\omega_1-\omega_2)$ between two equally populated ground states, $\rho_{gg}^{(0)}=\rho_{g'g'}^{(0)}=\frac{1}{2}$.

damping or if $\Gamma_{n'g}+\Gamma_{gn}-i\Gamma_{n'n}=0$. This last condition holds if the states $|n'\rangle$ and $|n\rangle$ can decay only by spontaneous emission to the ground state $|g\rangle$. This fact was also noted by Hansch and Toschek.[12] In this case the extra resonances will only be induced by other damping mechanisms, such as collisional mechanisms for which $\Gamma_{gn}+\Gamma_{n'g}-\Gamma_{n'n}\neq 0$.

In media with inversion symmetry there is no dipole moment associated with $\rho^{(2)}_{n'n}$, and no difference frequency is generated. The existence of this coherence may be demonstrated in a four-wave mixing experiment. The presence of the two incident waves sets up a coherence grating $\rho^{(2)}_{n'n}\exp[i(\vec{k}_1-\vec{k}_2)\cdot\vec{r}-i(\omega_1-\omega_2)t]$, from which a third wave may be scattered to generate a fourth wave. The existence of such a collision-induced coherence, or pressure-induced extra resonance, was first demonstrated by four-wave mixing in a system of Na vapor and helium buffer gas.[8] In this case $|g\rangle$ corresponds to the $3S_{1/2}$ ground state and $|n\rangle$ and $|n'\rangle$ to the doublet $3P_{3/2,1/2}$. A detailed comparison between theory and experiment[11,13] confirmed the correct treatment of damping in nonlinear situations.

Another way to describe the same phenomenon utilizes the concept of dressed material states. Grynberg[14] has shown that collisional transfer of population between dressed states leads to the same coherence given by Eq. (2) (as the collision acts only on the material part and not on the radiative part of the dressed eigenstates). An advantage of this method is that it can be extended to the case of large detunings. In this quasistatic regime details of the atomic interaction potential are important, and the Lorentzian line shapes characteristic of the impact approximation are no longer valid.

There are, however, differences between single-atom collisional redistribution and coherent four-wave mixing which require care in using this analogy. Most notably, the cooperative nature of four-wave mixing leads to phase-matching requirements and a different pressure dependence than for collisional redistribution. Different behaviors of the strengths of these processes with detuning from intermediate resonances have also been predicted.[15]

While there remains no ambiguity or disagreement about the correctness of Eq. (2) to describe the coherence $\rho^{(2)}_{n'n}$ in the impact approximation, the verbal interpretation has given rise to some discussion. If the material system contains other states besides the three levels depicted in Fig. 1, and if spontaneous emission from one or more of these three levels to those other states can occur, then the "extra resonance" would be observable even in the absence of collisions. In this case it would be more rigorous to speak of collision-enhanced coherence.[16] In fact, the extra resonance could then also be enhanced by thermal radiation fields, which would cause an increase in $\Gamma_{n'g}+\Gamma_{gn}-\Gamma_{n'n}$. Enhancement by higher-order radiative processes has also been considered theoretically.[17]

Enhancement of the resonance between two initially unpopulated vibrational states of an electronically excited manifold has been observed for the molecules embedded in a host crystal at low temperature.[18,19] The four-wave mixing resonance was observed to increase in intensity as the temperature was increased. This increased the numerator $\Gamma_{n'g}+\Gamma_{ng}-\Gamma_{n'n}$, as the damping due to phonon interactions is increased. Such experiments may provide a new tool to study relaxation processes of molecules in excited electronic configurations.

It is, of course, somewhat paradoxical that the occurrence of collisions can give rise to, or enhance, the intensity of a coherent light beam in a four-wave mixing process. This fact may be made understandable by observing that there are two channels leading from Eq. (1a) to the coherence $\rho^{(2)}_{n'n}$ in Eq. (2). In the absence of damping there is a destructive type of interference between these two coherent pathways. The presence of collisions *destroys* this *destructive* interference.[11] Despite a contrary view expressed by Dagenais,[20] we believe this is a logically satisfying description of the physical situation. A somewhat analogous situation may occur in two-photon absorption processes or in Raman scattering. Bjorkholm and Liao[21] have shown that, for the two-photon transition from the $3S_{1/2}$ to the $3D_{3/2}$ states in Na vapor, destructive interference occurs if one laser frequency is tuned between the D_1 and D_2 resonances of the Na doublet. The intermediate states $3P_{1/2}$ and $3P_{3/2}$ will give opposing contributions to the two-photon matrix element because of the opposite sign of the detuning denominators. This destructive interference is essentially complete for one particular choice of ω_1. If now a buffer gas is added and collisions cause the imaginary part of the respective denominators to become significant, this destructive interference will be reduced. It will disappear completely if the doublet resonances are broadened to significant overlap. Although we made an attempt to demonstrate it, experimental difficulties have prevented us from positively identifying this effect. It would be another example of a collision-induced effect on $\chi^{(3)}$. The two effects, which are closely related but not identical, have been discussed in detail by Yee and Fujimoto[22] with the aid of double-sided Feynman diagrams.

It is well known that second-order perturbation theory gives rise to changes in the diagonal elements of the density matrix.[23–25] In fact, $\rho^{(2)}_{gg}$ and $\rho^{(2)}_{nn}$ or $\rho^{(2)}_{n'n'}$ will show sharp resonances for $\omega_1-\omega_2=0$ with a width equal to the inverse lifetime of these states. Bogdan *et al.* have demonstrated collision-induced population gratings.[25] We have studied such gratings at high resolution for a variety of buffer gases. These results will be the subject of a separate publication.

Dagenais[16] has emphasized that the Schwarzschild-type inequality $|\rho^{(2)}_{nn'}|^2\leq\rho^{(2)}_{nn}\rho^{(2)}_{n'n'}$ must always be obeyed. This does not imply, however, that $\rho^{(2)}_{nn'}$ is *caused* by the population changes or could be theoretically derived from them. Population changes and coherences are concomitant but independent phenomena. Their relative independence is best illustrated by the frequency dependence of $\rho^{(2)}_{n'n}$, which has a resonance as ω_2 is swept through $\omega_1\pm\omega_{n'n}$, while the populations remain essentially constant.

A careful distinction should also be made between $\chi^{(3)}$ effects and collision-induced effects of higher order, where first excited states are populated with collisional assistance and subsequently four-wave mixing experiments are performed. Such effects are properly described by

nonlinear susceptibilities of higher order.

This paper is concerned with coherences between two states belonging to the ground-state manifold, as depicted in Fig. 1(b). Such coherences can also be detected by four-wave mixing and they are also induced or enhanced by collisions.[11,15] The second-order coherence between two initially populated states of the ground-state manifold is given by

$$\rho_{gg'}^{(2)}(\omega_1-\omega_2)=\frac{\mu_{ng}\mu_{g'n}E_1E_2^*}{4\hbar^2[\omega_{g'g}-(\omega_1-\omega_2)-i\Gamma_{g'g}]}\times\left[\frac{\rho_{gg}^{(0)}}{\omega_1-\omega_{eg}-i\Gamma_{eg}}+\frac{\rho_{g'g'}^{(0)}}{\omega_{eg'}-\omega_2-i\Gamma_{eg'}}\right]. \tag{3}$$

At the Raman resonance condition $\omega_{g'g}=\omega_1-\omega_2$, which implies equal detunings $\Delta=\omega_1-\omega_{eg}=\omega_2-\omega_{eg'}$, this expression reduces, for the case $\Gamma_{eg}=\Gamma_{eg'}=\Gamma$ and for large detuning $\Delta\gg\Gamma$, to

$$\rho_{gg'}^{(2)}=\frac{\mu_{ng}\mu_{g'n}E_1E_2^*}{4\hbar^2[\omega_{g'g}-(\omega_1-\omega_2)-i\Gamma_{g'g}]}\times\left[\frac{\rho_{g'g'}^{(0)}-\rho_{gg}^{(0)}}{\Delta}+\frac{i\Gamma(\rho_{g'g'}^{(0)}+\rho_{gg}^{(0)})}{\Delta^2}\right]. \tag{4}$$

The first term vanishes when the two levels $|g\rangle$ and $|g'\rangle$ have equal populations. This is the basis of the conventional statement that the Raman-type susceptibility between two equally populated levels vanishes. In the presence of damping, the second term, which is proportional to the sum of the populations in the two levels, can be significant. It exists even in the absence of collisions, when Γ is determined by spontaneous emission. When collisional broadening is dominant, the coherence will be proportional to the buffer-gas pressure. Bogdan *et al.*[25] already reported a collision-enhanced resonance in four-wave mixing for the case that $|g\rangle$ and $|g'\rangle$ stand for the $F=1$ and $F=2$ hyperfine levels of the $3^2S_{1/2}$ ground state of the Na atom. This resonance occurs when $\omega_1-\omega_2=1772$ MHz. It could obviously be very sharp because the damping $\Gamma_{gg'}$ between two components of the electronic ground state is determined by magnetic spin-flip interactions, but the resolution in this first experiment was insufficient to make a detailed study of mechanisms determining the linewidth.

It is also possible that $|g\rangle$ and $|g'\rangle$ correspond to two Zeeman sublevels with different spatial quantum numbers m and m'. In the presence of an external magnetic field such levels would not be degenerate. Grynberg first called attention to collision-induced Zeeman coherences.[26] We have reported the observation of such resonances in the $3^2S_{1/2}$ ground-state configuration of Na atoms, mixed with various buffer gases.[27]

Here results of more recent, higher resolution studies are reported for the Zeeman and hyperfine coherences. In Sec. II the experimental arrangement is reviewed. The intensity and the width of the resonances are studied as a function of the pressure of various buffer gases in Sec. III. Residual Doppler broadening and collisional narrowing by various types of velocity-changing collisions, as well as the causes for the ultimate homogeneous broadening, are discussed.

In Sec. IV the resonances are studied as a function of an externally applied magnetic field for various configurations of the polarizations of the three incident light beams and the direction of the external field. Selection rules are presented which permit a distinction between Zeeman coherences and population gratings even in the absence of a magnetic field. The relationship to the collision-induced Hanle effect is pointed out in Sec. V.

II. EXPERIMENT

The experimental apparatus is similar to that used in previous studies of collision-induced four-wave mixing.[11,13,27] A schematic of the apparatus is diagramed in Fig. 2. The present experiment uses two argon-ion laser-pumped (Spectra Physics Model 171-19, 6W at 514 nm), single-mode, continuously tunable cw dye lasers (Coherent 599-21). These are frequency stabilized with active feedback electronics to a root-mean-square linewidth of approximately 2 MHz, which represents an improvement of more than an order of magnitude over previous experiments. The output of each laser is monitored with a 7.5-GHz free spectral-range-scanning Fabry-Perot etalon with 40-MHz resolution. One laser, taken to have frequency ω_1, is split into two beams which are made to propagate parallel to one another but are offset by 1—5 mm. The beam from the second laser at ω_2 propagates parallel to each of these, so that in a plane perpendicular to the direction of travel the three beams fall at three corners of a square with the beam at ω_2 occupying the intermediate vertex.

The three Gaussian beams are each about 1 mm in diameter and are focused to the center of a 10-cm-long stainless-steel sodium heat pipe by a 5-cm focal-length lens which is the entrance "window" of the oven. The beam diameters at the focus are approximately 20 μm. Here the beams with wave vectors $\vec{k}_1$ and $\vec{k}_2$ cross each other at an angle which could be varied in the range of 1°—6°. The beams are recollimated by a matching 5-cm focal-length lens which is the exit window. This scheme enforces a three-dimensional phase-matching geometry[28—30] which enables spatial discrimination of the

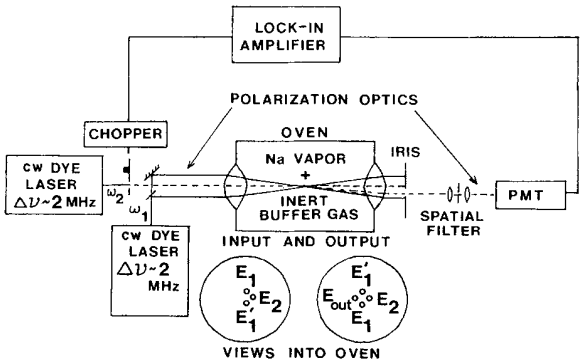

FIG. 2. Schematic of experimental apparatus. PMT is the photomultiplier tube.

generated wave from the input beams even if the beams have nearly or exactly the same frequency. Good phase matching over a wide range of tunability is obtainable, which is not possible in the conventional phase-conjugate backward wave geometry of frequency degenerate four-wave mixing.

The input beams are blocked at the heat pipe exit and the signal beam is transmitted through a pinhole and spatial filter to a photomultiplier tube operated at low gain. Additional discrimination against scattered light from the beams at ω_1 is provided by mechanically chopping the beam at ω_2 and by using phase-sensitive detection (PAR HR-8 lock-in amplifier). Each of the three input beams has linear polarization which can be rotated with a half-wave retarder or made circular with a Fresnel rhomb. For some combinations of input polarizations a polarizer preceding the photomultiplier provides additional discrimination against scattered light. It is possible to rotate the double Fresnel-rhomb half-wave retarders without appreciably altering the beam alignment.

Nichrome-wire heaters with variable ac current heat the oven to between 200 and 300 °C, corresponding to sodium densities in the neighborhood of 10^{13}–10^{14}/cm^3. Inert buffer gases (He, Ar, Xe, N_2) are added in pressures up to 3 atm, as measured by a capacitance manometer (MKS Baratron 170M). Addition of buffer gases can affect the density of sodium in the interaction region.[31] In principle, measuring the nonresonant four-wave mixing intensity can be used to correct for variations in sodium density and laser intensity. At the small angles used in most of the experiments ($<2°$), the nonresonant background is difficult to measure accurately due to scattering noise. In studies where cesium admixtures are also present, solid cesium is added into the heat pipe with the sodium metal. The cesium pressure is governed by the oven temperature where it is placed and cannot be varied independent of the sodium pressure. Addition of cesium also strongly affects the density of sodium in the interaction region.

The lasers are detuned either below the D_1 ($3^2S_{1/2}$-$3^2P_{1/2}$) line or above the D_2 ($3^2S_{1/2}$-$3^2P_{3/2}$) line of sodium by about $\Delta=30$ GHz (1 cm^{-1}), a value small enough to make only one of the $3P$ levels near resonant. This detuning is, however, very large compared to the Doppler width ($\Delta\nu_D\approx 2$ GHz), the Rabi frequency ($\nu_R\approx 10$–100 MHz at typical intensities), and the collisional width T_2^{-1} (full width at half maximum approximately equal to 11 MHz per Torr of He buffer-gas pressure). Thus, no particular velocity group is selected, no one-photon saturation effects are important, and only a small amount of absorption occurs, all collisionally assisted. Because all of the beams have nearly the same frequency $\bar{\omega}\approx\omega_{3S\text{-}3P}$ and because $2\bar{\omega}$ is not near any sodium resonances, the only contributions to $\chi^{(3)}$ resonant in all three energy denominators are those where the output frequency ω_{out} is also near $\bar{\omega}$. The only phase-matched combination in the cited experimental geometry is that with $\omega_{\text{out}}=2\omega_1-\omega_2$ and $\vec{k}_{\text{out}}=\vec{k}_1+\vec{k}'_1-\vec{k}_2$ where $\vec{k}_1$ and $\vec{k}'_1$ denote wave vectors of the two beams at ω_1. The laser with frequency ω_1 is scanned to higher frequency with ω_2 fixed to observe four-wave mixing resonances in the difference frequency $\omega_1-\omega_2$. The scan rate is calibrated by measuring resonances known to be separated by the ground-state hyperfine splitting of sodium.

III. LINE SHAPE AND INTENSITY OF COLLISION-INDUCED ZEEMAN COHERENCES

The intensity $I(2\omega_1-\omega_2)$ of the newly generated output wave is proportional to $|\chi^{(3)}|^2$, the absolute square of the pertinent third-order susceptibility. The dominant term is derived from the second-order coherence in Eq. (4),

$$\chi^{(3)}(-2\omega_1+\omega_2;\omega_1,-\omega_2,\omega_1)=\int_{-\infty}^{+\infty}\frac{\mu_{ge}\mu_{eg'}\mu_{g'e}\mu_{eg}N_0(+i\Gamma)}{\hbar^3\Delta^3[\omega_{g'g}-(\omega_1-\omega_2)-(\vec{k}_1-\vec{k}_2)\cdot\vec{v}+i\Gamma_{g'g}]}f(\vec{v})d\vec{v}\ . \tag{5}$$

Here N_0 is the number of Na atoms per cm^3 and $f(\vec{v})$ is a distribution over suitably averaged atomic velocities. The Doppler shift in the Raman-type resonant denominator has been explicitly included. The other denominators have been set equal to the detuning Δ, which is large compared to the damping and the Doppler shift of one-photon transitions, $\Delta\gg\Gamma_{eg}$, $|\vec{k}_1\cdot\vec{v}|$. A complete treatment of Doppler broadening in four-wave mixing, when the detuning is small, has been published.[32] In this case, particular velocity groups are singled out and selective absorption occurs, which leads to complications in the interpretation of the collision-induced signals.

The complete energy-level diagram of the $3S$ and $3P$ configurations of the Na atom in a weak external magnetic field, shown in Fig. 3, is of course much more complex than the three-level simplifications of Fig. 1. Since the hyperfine splitting in the excited P states is small compared to the detuning, the summation over the virtual excited states $|n\rangle$ can be restricted to one 3^2P configura-

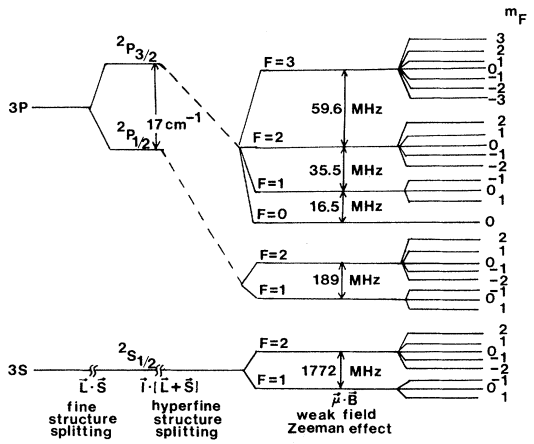

FIG. 3. Energy levels of the 3^2S and 3^2P configurations of Na.

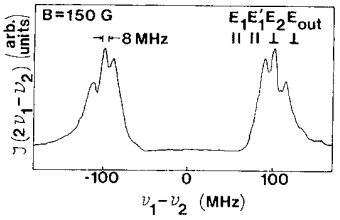

FIG. 4. Collision-induced Zeeman resonances in four-wave mixing in an external magnetic field ($p_{He}=700$ Torr, $\Delta=30$ GHz below $3^2P_{1/2}$).

tion, and a common average value of Δ can be used for all its sublevels. Since all the dipole matrix elements connecting the pertinent excited states with any sublevel $|g\rangle$ or $|g'\rangle$ of the ground state are known, $\chi^{(3)}$ can be calculated theoretically from Eq. (5).

In Fig. 4 we have shown the nearly degenerate four-wave mixing resonance in an external field $B=175$ G in a mixture of Na vapor at 30 mTorr with a helium buffer-gas pressure of 700 Torr. The magnetic field was applied perpendicular to the direction of propagation of the light beams, parallel to the $\vec{E}$ fields of the beams at ω_1, and perpendicular to the polarization of the beam at ω_2. We shall discuss details of the selection rules under these conditions in Sec. IV. The absence of the resonance at $\omega_1=\omega_2$ is experimentally evident. No population gratings contribute to the signal in this polarization geometry. Only Zeeman coherences are observed due to $\rho^{(2)}_{mm'}$ with $m'=m\pm1$. The pattern agrees well with the computer-generated response using Eq. (5), which is reproduced in Fig. 5.

If the external magnetic field is reduced to zero, the Raman-type resonances of the Zeeman coherence collapse to a single line with $\omega_{gg'}=\omega_1-\omega_2=0$. Figure 6 shows that this resonance has a width of 4 MHz, considerably narrower than the one-photon spontaneous linewidth $\Gamma\approx\Gamma_{ge}\approx10$ MHz and also narrower than the collision-free Doppler width

$$\Delta\omega_D=(\vec{k}_1-\vec{k}_2)\cdot\vec{v}\approx2\vec{k}_1\,|\,v\,|\sin(\tfrac{1}{2}\theta)\,, \tag{6}$$

where θ is the angle between the wave vectors $\vec{k}_1$ and $\vec{k}_2$.

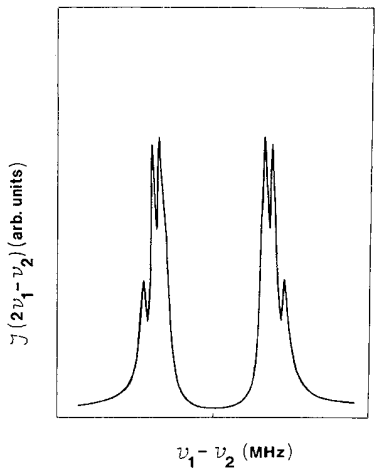

FIG. 5. Computer simulation of the data in Fig. 4.

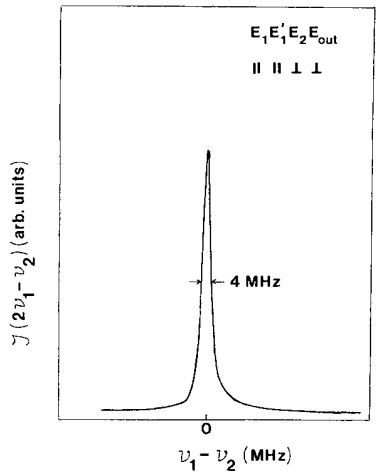

FIG. 6. Zeeman coherences in vanishing magnetic field.

A. Collisional narrowing of Doppler broadening

At the helium pressure of 700 Torr this inhomogeneous Doppler broadening is much reduced because of collisional narrowing. During the time $\Delta\omega_D^{-1}$, a Na atom undergoes many collisions which average out the velocity. Call the time required for a significant change in velocity, i.e., the velocity correlation time, τ_c, which is inversely proportional to the pressure. Then we have at high pressures, $\tau_c\Delta\omega_D\ll1$, the reduced width

$$\Delta\omega_r\approx\Delta\omega_D^2\tau_c\,. \tag{7a}$$

One may also describe the motional narrowing of the Doppler broadening in the spatial domain. A coherence grating is created with a spacing $\pi\,|\,\vec{k}_1-\vec{k}_2\,|^{-1}$. If collisions prevent significant diffusion of the Na atoms, because the mean free path $l=\tau_c v$ is small compared to the grating constant, motional narrowing of $\Delta\omega_D$ will occur. The limiting behavior for $l\,|\,\vec{k}_1-\vec{k}_2\,|\ll1$ yields a residual Doppler contribution

$$\Delta\omega_r=\Delta\omega_D l\,|\,\vec{k}_1-\vec{k}_2\,| \tag{7b}$$

which is equivalent to Eq. (7a). The mean free path is related to the cross section by

$$l=\frac{1}{n\sigma_0}\frac{\bar{v}}{\bar{V}}\,, \tag{8}$$

where n is the number density of the inert gas, σ_0 the velocity-changing collision cross section between sodium and inert gas atoms, $\bar{V}$ the average relative velocity, and $\bar{v}$ the average thermal speed of the Na atom.

We have experimentally observed that the width depends on the angle between the beams at low buffer-gas pressures and that it narrows with increasing helium pressure. These data are displayed in Figs. 7 and 8. Note that the narrowing sets in at lower pressures, the smaller the angle θ. At high pressures the broadening is indeed inversely proportional to the pressure, in agreement with Eqs. (7a) or (7b).

Elimination of Doppler broadening in microwave reso-

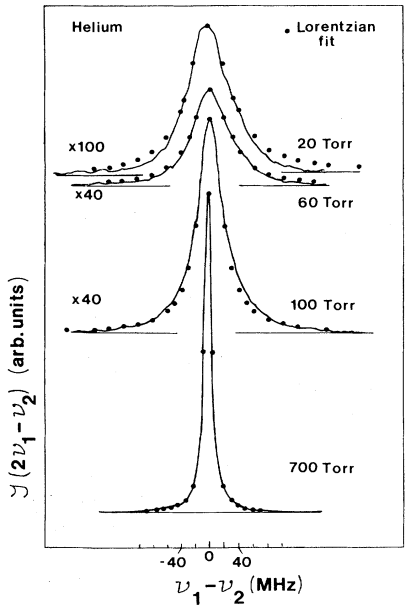

FIG. 7. Line shapes of Zeeman coherence resonances in Na-He mixture for $\theta=3°$.

nances was first proposed by Dicke, and the reduction in inhomogeneous width was first observed by Romer and Dicke[33] with wall collisions in a very small cavity. Soon thereafter narrowing by the addition of a buffer gas in a large cavity was observed.

Heretofore, collisional narrowing has never been observed on pure electronic transitions since such transitions usually are broadened by the optical dephasing induced by the collisions. This causes a homogeneous broadening which obscures the collisional narrowing of the Doppler width. The observation of Doppler narrowing in optical spectroscopy has previously been confined to infrared and Raman spectra of vibrational and rotational transitions in small molecules. Even there the dissimilarity in collisional potentials for the transition levels is sufficient to restrict experiments to light molecules, so that velocity-changing effects are dramatic. Most experiments to date

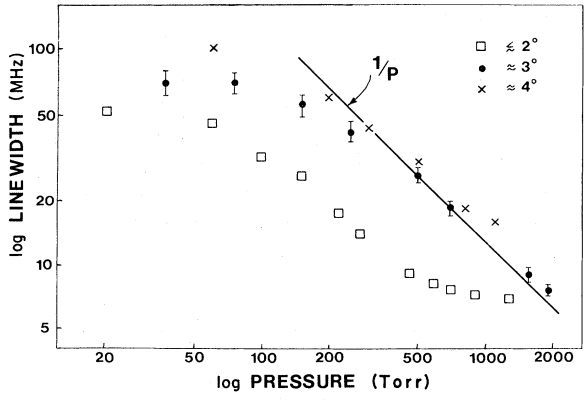

FIG. 8. Linewidth as a function of helium pressure for three angles θ.

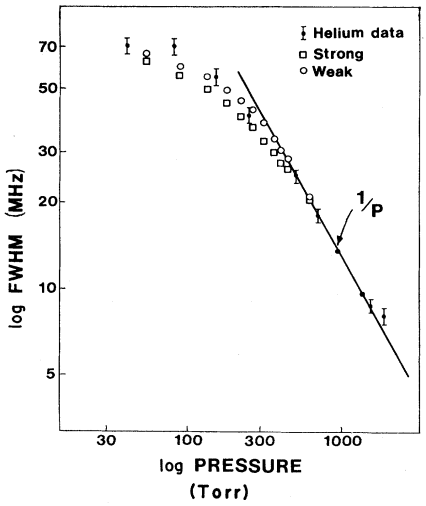

FIG. 9. Comparison of collisional narrowing in helium with models of strong and weak velocity-changing collisions.

have been on narrowing in H_2, D_2, and HD, and a brief survey is given by Pine.[34]

In our four-wave mixing experiments collisional dephasing is absent since the Zeeman levels $|g\rangle$ and $|g'\rangle$ have essentially the same interaction potential during the collisions. Therefore, the collisions in our case behave as pure velocity-changing collisions. They may be incorporated in the classical Boltzman transport equation

$$\frac{\partial f}{\partial t}+\vec{v}\cdot\vec{\nabla}f=\left[\frac{\partial f}{\partial t}\right]_{\text{coll}}.$$

This permits a comparison of theoretical models of Doppler narrowing with our experimental results.

Rautian and Sobel'man[35] have discussed the influence of velocity-changing collisions on one-photon absorption and fluorescence line shapes in the limiting cases of the strong collision and weak collision models. In the former, each collision essentially rethermalizes the atomic velocity; in the latter, the velocity change in a single collision is relatively small. The predicted line shapes are Lorentzian

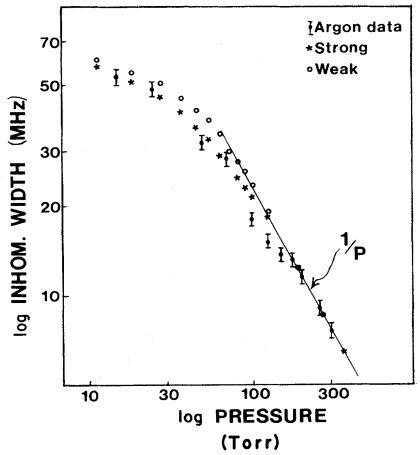

FIG. 10. Comparison of collisional narrowing in argon with models of strong and weak velocity-changing collisions.

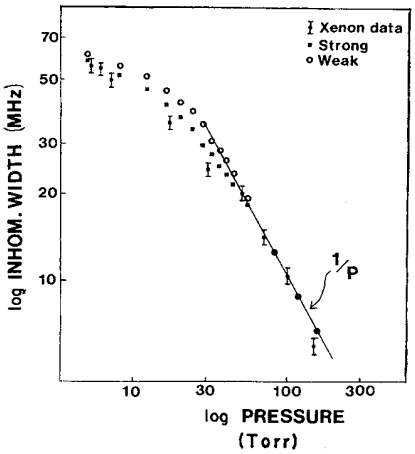

FIG. 11. Comparison of collisional narrowing in xenon with models of strong and weak velocity-changing collisions.

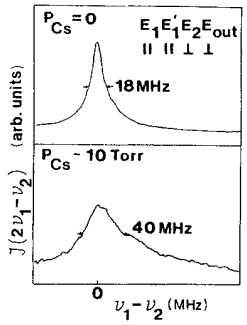

FIG. 12. Broadening of Zeeman coherence resonance by Na-Cs spin-exchange collisions.

at high pressures, while the wings are suppressed at lower pressures. In the absence of collisions the Gaussian shape of the Doppler broadening is recovered. Details of the line shape in the intermediate narrowing regime are model dependent.

In Figs. 9—11 we compare our experimental results for three different buffer gases, He, Ar, and Xe, respectively, with the theoretical predictions. The vertical placement of the theoretical curves on the data is determined by the measured collision-free Doppler width, and the horizontal placement is specified by the coincidence of the $1/p$ limiting dependence of the linewidth. Clearly, collisions with successively heavier collision partners tend to agree better with those described by a strong collision model. The values of averaged velocity-changing collision cross sections derived from Eqs. (7b) and (8) are 2.3×10^{-15} cm^2 in He, 6.1×10^{-15} cm^2 in Ar, and 1.0×10^{-14} cm^2 in Xe to about $\pm20\%$. Diffusion coefficients are easily obtained from these cross sections for a given foreign-gas pressure.

B. Residual linewidth

While the Doppler contribution to the width can be effectively eliminated by working with small angles θ between the beam at high buffer-gas pressure, the data in Fig. 8 reveal that there remain other contributions to the observed width. The asymptotic value at high pressures of about 7 MHz in this figure is higher than the 4-MHz width shown in Fig. 6. The difference is due to power broadening since the data in Fig. 8 were taken at higher beam intensities. No further narrowing of the linewidth below 4 MHz could be obtained by lowering the power level still further. We believe the residual width of 4 MHz is of instrumental origin due to frequency jitter of the two lasers, each being stabilized to approximately 2 MHz. The true homogeneous width of the resonance, $\Gamma_{g'g}$, should be considerably smaller. The dominant contribution of $\Gamma_{g'g}$ is expected to result from spin-exchange collisions between pairs of Na atoms. Such collisions can cause transitions between Zeeman and hyperfine levels. They have been studied extensively in radiofrequency spectroscopy studies.[36] At the Na pressure prevailing in our experiment, and from the known spin-exchange collision cross section, $\Gamma_{g'g}$ is expected to lie in the range of 50—300 kHz.

It is difficult to change the Na vapor pressure because this changes the index of refraction of the sample and hence the beam overlap and absorption in the cell. In order to demonstrate that spin-exchange collisions contribute to the homogeneous width, we have added Ca vapor to our cell, keeping the oven temperature constant. Figure 12 shows a significant broadening at 10 Torr of Cs pressure. The observed increase in width due to the Cs-Na spin-exchange collisions is in agreement with the estimate of the cross section for this process and the prevailing densities. The asymmetry is tentatively ascribed to interference with a nonresonant background contribution to $\chi^{(3)}$ from the rather high Cs density. Furthermore, the Na density may be affected by the formation of CsNa molecules. The data in Fig. 11 have therefore only a semiquantitative character. They confirm the nature of the homogeneous broadening $\Gamma_{gg'}$.

C. Intensity dependence on buffer-gas pressure and detuning

The intensity of the resonant signal at the line center increases with buffer-gas pressure, as indicated in Fig. 13. At pressures below the onset of collisional narrowing, the linewidth is constant and equal to $\Delta\omega_D$. At very high pressures the linewidth is again constant and equal to the instrumental width. In these pressure ranges the peak intensity is proportional to the square of the buffer-gas pressure p_{He}. This is in agreement with Eq. (4), since $\Gamma=\Gamma_{gn}$ is proportional to p_{He}, and therefore $|\chi^{(3)}|^2$ to p_{He}^2, according to Eq. (5). At intermediate pressures the peak intensity increases at p_{He}^3. In this regime the linewidth changes inversely proportional to p_{He}, due to collisional Doppler narrowing. While the integrated resonant signal remains proportional to p_{He}^2, the peak intensity increases as p_{He}^3.

At very high buffer-gas pressures, beyond the range shown in Fig. 13, the intensity starts to level off and finally decreases with pressure. This happens when the collisional absorption width Γ_{gn} becomes comparable to the detuning Δ and the incident beams undergo considerable absorption.

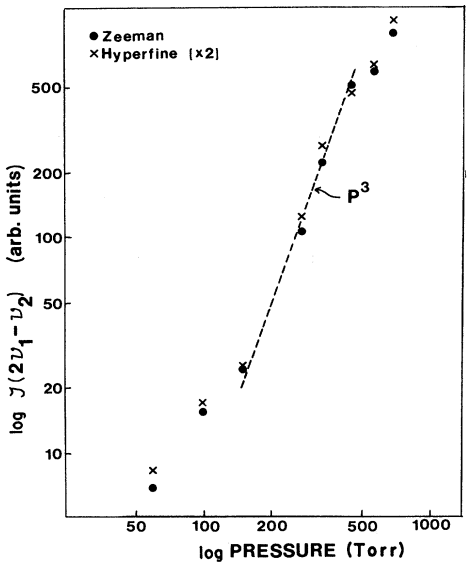

FIG. 13. Pressure dependence of the peak intensity of Zeeman coherence resonance.

Another characteristic of the third-order susceptibility describing the collision-induced Raman-type Zeeman coherence is its proportionality to Δ^{-3}. Ordinarily Raman-type susceptibilities are proportional to Δ^{-2}. We have verified that the intensity of the collision-induced resonances varies as Δ^{-6} for detunings satisfying the impact approximation ($\Delta \ll 1/\tau_{\text{coll}}$, where τ_{coll} is the duration of a collision). Unfortunately, our signals become too small to test interesting theoretical predictions in the quasistatic regime ($\Delta \gg 1/\tau_{\text{coll}}$), where details of the interatomic potential becomes important.

IV. SELECTION RULES FOR ZEEMAN AND HYPERFINE COHERENCES

In a weak magnetic field the eight states of the $3^2S_{1/2}$ fundamental level of Na^{23} with nuclear spin $I=\frac{3}{2}$ are nondegenerate and may be conveniently labeled by the set of quantum numbers $|F,m_F\rangle$, with $F=1$ or 2. Three types of contributions to the collision-induced four-wave mixing signals may be distinguished.

(1) Degenerate Zeeman resonances. Second-order perturbations in the diagonal elements of the density matrix $\rho^{(2)}_{F,m_F;F,m_F}$ cause degenerate frequency resonances at $\omega_1=\omega_2$. These transitions are characterized by $\Delta F=\Delta m_F=0$. They should be carefully distinguished from population-grating resonances, which occur because real collision-induced transitions to the $3P$ manifold may take place and cause a modulation of this excited-state population at $\omega_1-\omega_2$. The subsequent relaxation of these $3P$-state populations by spontaneous emission or by radiationless decay to the $3S$ manifold may also contribute to $\rho^{(2)}_{F,m_F;F,m_F}(\omega_1-\omega_2)$, modulated at the difference frequency $\omega_1-\omega_2$. It is quite clear that no population grating in this sense can be induced if the fields at ω_1 and ω_2 are mutually orthogonal. For conditions where fields at ω_1 and ω_2 have the same state of polarization, such population gratings contribute significantly to the four-wave mixing at $\omega_1-\omega_2=0$. These effects fall outside the scope of the present paper and will be discussed in detail elsewhere.[37] A similar distinction, based on polarization selection rules, was made by Steel *et al.*[38,39] The experiments of these authors, like those of Bloch *et al.*,[40–42] are carried out at resonance, $\Delta=0$ for one selected velocity group. Dephasing collisions still play an essential role. A phase-conjugate backward-wave geometry is used by these authors with $\omega_1=\omega_2$. The analysis and interpretation of the data is more complicated in those degenerate cases.

(2) Nondegenerate Zeeman-type resonances are caused by terms $\rho^{(2)}_{F,m_F;F,m_F'}$ at a frequency corresponding to an energy separation between two Zeeman levels ($m_F' \neq m_F$) of the same hyperfine state ($\Delta F=0$). An example was shown in Fig. 4.

(3) Hyperfine resonances are caused by terms $\rho^{(2)}_{F,m_F;F',m_F'}$, with $\Delta F=F'-F=\pm 1$. They are centered around the hyperfine splitting of the ground state $\omega_1-\omega_2 \approx 1.8$ GHz. Examples of this type of resonance are shown in Fig. 14.

The patterns in Figs. 4 and 14 obey the selection rule $\Delta m_F=m_F-m_{F'}=\pm 1$. The energy separation of such pairs of levels can be calculated from the Breit-Rabi hyperfine spin Hamiltonian. The effective Landé g values of the $F=1$ and 2 levels are $g_F=-\frac{1}{2}$ and $+\frac{1}{2}$, respectively. Thus, some resonances coincide in Fig. 14. In Fig. 4 the peak on the right ($\omega_1-\omega_2>0$) represents coherent anti-Stokes Raman-type Zeeman resonances and contains contributions of $\Delta m_F=+1$ within the $F=2$ manifold and $\Delta m_F=-1$ within the $F=1$ manifold. The substructure in these two peaks is a result of the breakdown of the weak-field (linear) Zeeman effect with the incipient Paschen-Back decoupling of the nuclear and electron spins. The energy separation between the maxima inside each sideband has the order of magnitude $(g\beta H_0)^2/\Delta_{\text{hfs}} \sim 5$ MHz. Since F and m_F are not exact quantum numbers, very weak satellite resonances should, in principle, exist. Since their intensity is down by a factor $(g\beta H_0/\Delta_{\text{hfs}})^2$, they were not observed. The pattern in Fig. 4 compares very well with a purely theoretical calculation in Fig. 5 based on the known electric dipole matrix elements connecting the various $|F,m_F\rangle$ states of the $3^2S_{1/2}$ configuration with the Zeeman sublevels of the excited $3^2P_{1/2}$ level. The agreement between theory and experiment not only confirms the selection rules, but also demonstrates that deviations due to the small angle between the beams and alignment of the magnetic field are negligible.

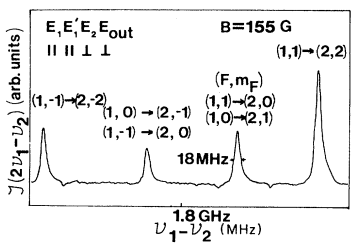

FIG. 14. Hyperfine coherence resonances ($\Delta F=1$, $|\Delta m_F|=1$).

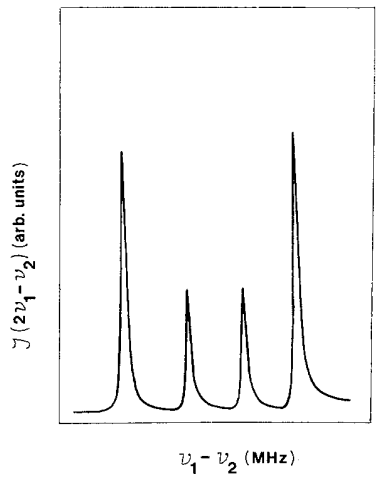

FIG. 15. Computer simulation of the data in Fig. 14.

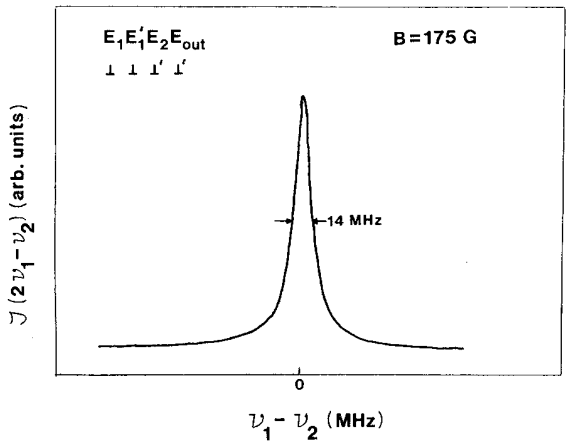

FIG. 17. Zeeman resonance with the external magnetic field and the electric fields at ω_1 and ω_2 mutually perpendicular.

The hyperfine coherence pattern in Fig. 14 should be compared with the computer calculation in Fig. 15. The cause of the observed experimental asymmetry in the intensity is not established, but it could be some optical-pumping mechanism. Whatever the cause, it should be counteracted by the addition of Cs vapor. The spin-exchange collisions would tend to reestablish an equilibrium population over all ground-state levels. A symmetrical intensity pattern of the hyperfine resonances is indeed observed in the presence of 10 Torr of Cs vapor, as shown in Fig. 16. Thus the agreement between theory and experiment may be considered satisfactory.

In general, one would expect a selection rule with $|\Delta m_F| \leq 2$ for Raman-type transitions. There are, however, severe restrictions, since both the initial and the final state of the two-phonon electric dipole transition belong to S-state orbitals. The Zeeman effect for two-photon transitions between the 3^2S and 5^2S states of Na was discussed some time ago. In that case there was a large detuning from the $3^2P_{1/2,3/2}$ doublet and a selection rule $\Delta M=0$ was established.[43] For our Raman-type transitions between two states of the same 3^2S manifold only one of the intermediate 3^2P configurations contributes. The selection rule $|\Delta m_F|=1$ for the polarization geometry used may be understood as follows.

The fields E_1 and E_1' at ω_1 are polarized parallel to the magnetic field, which is taken as the quantization axis. The field E_2 is polarized at right angles. Use a description in which the orbital state is decoupled from the electron spin and introduce the spin-orbit coupling $\lambda L_z S_z+\frac{1}{2}(L^+S^-+L^-S^+)$ as an explicit perturbation in the 3^2P manifold. The ground 3^2S state has, of course, $m_L=0$. The electric dipole perturbation at ω_1 only connects with states $m_L=0$, that at ω_2 only with states $m_L=\pm 1$ in the virtual excited $3P$ manifold. The spin-orbit coupling term $(L^+S^-+L^-S^+)$ admixes these orbital states. Thus this polarization permits a Raman-type electric dipole transition with $\Delta m_S=\pm 1$. Therefore, the selection rule $|\Delta m_F|=+1$ applies to both the Zeeman and the hyperfine coherences in this geometry.

We next turn to the case that the magnetic field is applied parallel to the direction of propagation of the light beam, while the electric fields at ω_1 and ω_2, respectively, are perpendicular to each other and to the magnetic field. With the axis of quantization parallel to the magnetic

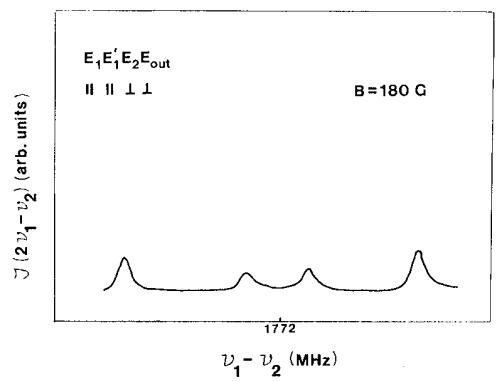

FIG. 16. Hyperfine coherence resonances, as in Fig. 14, but with the addition of 10 Torr Cs vapor.

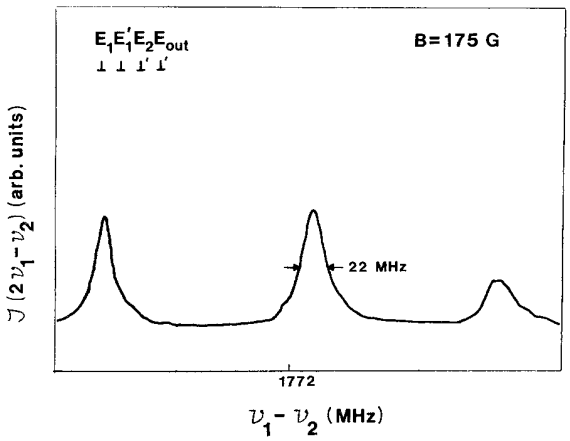

FIG. 18. Hyperfine resonances ($\Delta F=1$, $\Delta m_F=0$) in an external field parallel to the propagation direction.

TABLE I. Selection rules for collision-induced coherences in the $3S$ manifold of Na in a weak magnetic field by optical four-wave mixing.

Polarization of incident light beams			Zeeman coherence	Hyperfine coherence	Population grating
E_1	E_1'	E_2	$\rho^{(2)}_{F,m_F;F,m_F'}$	$\rho^{(2)}_{F,m_F;F',m_{F'}'}$	$\rho^{(2)}_{F,m_F;F,m_F}$
				$F'=F\pm1$	
$\parallel$	$\parallel$	$\perp$	yes, $m_F=m_F'\pm1$	yes, $m_{F'}'=m_F\pm1$	no
$\perp$	$\perp$	$\perp'$	yes, $m_F=m_F'$	yes, $m_{F'}'=m_F$	no
C	C	C	no	no	yes
C	C	C^*	no	no	no
$\parallel$	$\parallel$	$\parallel$	no	no	yes
$\parallel$	$\perp$	$\parallel$	yes, $m_F-m_F=\pm1$	yes, $m_{F'}'-m_F=\pm1$	yes

field, it is readily seen that the selection rule $\Delta m_F=0$ applies. The observed degenerate Zeeman coherence $\Delta F=\Delta m_F=0$ is shown in Fig. 17. The polarization geometry is indicated in the figure in self-explanatory notation. The three hyperfine coherences $|\Delta F|=1$, with $\Delta m_F=0$ for $m_F=m_{F'}=1,0,-1$, respectively, are shown in Fig. 18 for the same geometry, in which the external magnetic field is parallel to the direction of the light propagation.

If the incident light beams are circularly polarized in the same sense around the longitudinally applied magnetic field, a population grating is produced. The phases of the nonvanishing electric dipole matrix elements between the $3S$ and $3P$ manifolds are such that no (degenerate) Zeeman coherence is induced. If the sense of the circular polarization at ω_1 is opposite to that at ω_2, neither collision-induced population gratings nor Zeeman or hyperfine coherences occur. Transitions with $|\Delta m_F|=2$ are always forbidden.

Turning now to the case that the fields at ω_1 and ω_2 are all linearly polarized in the same direction, one finds that only population gratings are produced, regardless of the direction of an externally applied magnetic field. Finally, the hybrid case is considered, in which one beam at ω_1 is polarized parallel to that at ω_2 and parallel to an external field, but the other beam at ω_1 is polarized in an orthogonal direction. In this geometry, population gratings and Zeeman and hyperfine coherences exist simultaneously. The results of all these selection rules are summarized in Table I. We have experimentally confirmed the correctness of these rules for all listed geometries.

V. COLLISION-INDUCED HANLE EFFECT

In the limit that the external magnetic field goes to zero, the Zeeman resonances collapse to a single line at $\omega_1-\omega_2=0$ and the hyperfine resonances coalesce to a single line at $\omega_1-\omega_2=\Delta_{\rm hfs}$. The selection rules in the table remain valid in this limit. The discrepancy between the first two lines, which show selection rules $\Delta m_F=0$ and $|\Delta m_F|=1$, respectively, is only superficial. In the case of level degeneracy one has a choice which basis set of quantized states to adopt.

Consider again the Zeeman coherences in Fig. 4. It is clear that a similar pattern would have been obtained if the frequencies ω_1 and ω_2 had been held fixed, and the resonance at $\omega_1-\omega_2$ had been scanned by varying the external magnetic field. This is the usual procedure in magnetic-resonance spectroscopy. Next consider the case of Fig. 6. This resonance could have been scanned by holding $\omega_1=\omega_2$ constant and varying the external magnetic field through zero. This is usually known as a Hanle-type crossing experiment, which indicates a frequency degenerate Zeeman coherence. This establishes the close connection of our results with the collision-induced Hanle effect, which was first discussed theoretically by Grynberg.[26] It has been observed experimentally, using a pulsed laser, for a Zeeman coherence between sublevels of an electronically excited state in Ba vapor with argon buffer gas by Scholz *et al.*.[44] These authors were able to observe the resonance at large detunings Δ and to demonstrate the asymmetric nature of the detuning dependence of the four-wave mixing intensity in the quasistatic regime.

If $\omega_1-\omega_2$ is kept fixed at the value zero, all three incident light beams may be derived from a single laser. Furthermore, it is then also possible to use a standing-wave geometry, with a phase-conjugate backward wave as the output. This was, in fact, the geometry used by Scholz *et al.*[44] The Hanle-type degenerate Zeeman resonance can equally well be observed in our geometry and with high resolution continuous lasers. If the beams are derived from a single laser oscillator, the instrumental frequency jitter would be eliminated. One might expect to observe a much sharper resonance, with width $\Gamma_{gg'}$ set by the spin-exchange collision between Na atoms, rather than the 4 MHz residual width in Fig. 6. We are, at present, modifying our optical cell and adding Helmholtz coils to observe such zero crossings in collision-induced effects. A small fixed-frequency difference $\omega_1-\omega_2\lesssim100$ MHz could also be obtained from a single laser by using an acousto-optic modulator.

VI. CONCLUSIONS

The observation of collision-induced and collision-enhanced coherences has unequivocally established the correct treatment of damping in nonlinear, multiresonant situations. Collision-enhanced coherences between states of the electronic ground-state manifold exhibit resonances which are much narrower than the natural linewidth of the near-resonant intermediate one-photon transitions.

Optical four-wave mixing makes it possible to investigate resonances in the ground-state manifold with the same resolution as radiofrequency spectroscopy experiments in vapor cells. The observed spectra are in agreement with *ab initio* model calculations. Their *intensity* depends on optical dephasing constants Γ_{gn}.

Optical investigations of the collisional narrowing of Doppler-broadened profiles have yielded information about the nature of velocity-changing collisions between Na atoms and a variety of collision partners. It would be of interest to study collisional narrowing as a function of magnetic field and/or in the presence of depolarizing impurities.[40,45]

It may also be possible to study Raman transitions between rotational levels of heavy molecules, although the initial and final rotational states essentially have equal populations. The oscillator strengths are usually not as favorable as for Na atoms and high-intensity pulsed laser beams would probably be required. Collision-induced four-wave mixing provides a new tool to investigate various collisional processes in both excited and ground-state electronic configurations, as well as to study the spectroscopy of these manifolds.

ACKNOWLEDGMENT

This research was supported by the United States Joint Services Electronics Program under contract No. N00014-75-C-00648.

*Present address: AT&T Bell Laboratories, 1D317, 600 Mountain Avenue, Murray Hill, NJ 07974.

[1]N. Bloembergen, *Nonlinear Optics* (Benjamin, New York, 1965), p. 29.
[2]N. Bloembergen, H. Lotem, and R. T. Lynch, Jr., Indian J. Pure Appl. Phys. **16**, 151 (1978).
[3]S. A. J. Druet, B. Attal, T. K. Gustafson, and J. P. Taran, Phys. Rev. A **18**, 1529 (1978).
[4]S. A. J. Druet and J. P. Taran, in *Progress in Quantum Electronics,* edited by T. S. Moss and S. Stenholm (Pergamon, Oxford, 1981), Vol. 7, p. 1, and references quoted therein.
[5]P. N. Butcher, Nonlinear Optical Phenomena, Ohio State University Engineering Bulletin No. 200, 1965 (unpublished).
[6]A. Yariv, IEEE J. Quantum Electron. **QE-13**, 943 (1977).
[7]L. A. Carrera, L. P. Goss, and T. B. Malloy, J. Chem. Phys. **68**, 855 (1978).
[8]Y. Prior, A. R. Bogdan, M. Dagenais, and N. Bloembergen, Phys. Rev. Lett. **46**, 111 (1981).
[9]S. Y. Yee and T. K. Gustafson, Phys. Rev. A **18**, 1597 (1978).
[10]Y. Prior, IEEE J. Quantum Electron. **QE-20**, 37 (1984).
[11]N. Bloembergen, A. R. Bogdan, and M. W. Downer, in *Laser Spectroscopy V,* edited by A. R. W. McKellar, T. Oka, and B. P. Stoicheff (Springer, Heidelberg, 1981), p. 157.
[12]T. W. Hansch and P. Toschek, Z. Phys. **236**, 213 (1970). See also T. W. Hansch, in *Nonlinear Spectroscopy,* edited by N. Bloembergen (North-Holland, Amsterdam, 1977), p. 17.
[13]A. R. Bogdan, M. Downer, and N. Bloembergen, Phys. Rev. A **24**, 623 (1981).
[14]G. Grynberg, J. Phys. (Paris) B **14**, 2089 (1981).
[15]V. Mizrachi, T. Prior, and S. Mukamel, Opt. Lett. **8**, 145 (1983).
[16]M. Dagenais, Phys. Rev. A **26**, 869 (1982).
[17]H. Friedmann and A. D. Wilson-Gordon, Phys. Rev. A **26**, 2768 (1982); **28**, 302 (1983).
[18]J. R. Andrews, R. M. Hochstrasser, and H. P. Trommsdorff, Chem. Phys. **62**, 87 (1981).
[19]H. Levinsky and D. A. Wiersma, Chem. Phys. Lett. **92**, 24 (1982).
[20]M. Dagenais, Ref. 16, p. 875.
[21]J. E. Bjorkholm and P. F. Liao, Phys. Rev. Lett. **33**, 128 (1974).
[22]T. K. Yee and J. G. Fujimoto, Opt. Commun. **49**, 376 (1984).
[23]T. Yajima, H. Souma, and Y. Ishida, Phys. Rev. A **17**, 324 (1978).
[24]J-L. Oudar and Y. R. Shen, Phys. Rev. A **22**, 1141 (1980).
[25]A. R. Bogdan, M. W. Downer, and N. Bloembergen, Opt. Lett. **6**, 348 (1981).
[26]G. Grynberg, Opt. Commun. **38**, 439 (1981).
[27]N. Bloembergen, M. C. Downer, and L. J. Rothberg, in *Atomic Physics 8,* edited by I. Lindgren, A. Rosen, and S. Svanberg (Plenum, New York, 1983), p. 71; N. Bloembergen and L. J. Rothberg, in Coherence in Quantum Optics, edited by L. Mandel and E. Wolf (Plenum, New York, in press).
[28]S. Chandra, A. Compaan, and E. Wiener-Avnear, Appl. Phys. Lett. **33**, 867 (1978).
[29]A. C. Eckbreth, Appl. Phys. Lett. **32**, 421 (1978).
[30]Y. Prior, Appl. Opt. **19**, 1741 (1980).
[31]N. Allard and J. Kielkopf, Rev. Mod. Phys. **54**, 1103 (1983).
[32]S. A. J. Druet, J. P. Taran, and Ch. J. Borde, J. Phys. (Paris) **40**, 841 (1979).
[33]R. H. Romer and R. H. Dicke, Phys. Rev. **99**, 532 (1955).
[34]A. S. Pine, J. Mol. Spectrosc. **82**, 435 (1980).
[35]S. G. Rautian and I. I. Sobel'man, Usp. Fiz. Nauk. **90**, 209 (1966) [Sov. Phys.—Usp. **9**, 701 (1967)].
[36]W. Happer, Rev. Mod. Phys. **44**, 169 (1972).
[37]L. J. Rothberg and N. Bloembergen (unpublished). A brief account may be found in *Laser Spectroscopy VI,* edited by H. P. Weber and W. Luthy (Springer, Heidelberg, 1983), p. 178.
[38]D. G. Steel, J. F. Lam, and R. A. McFarlane, in *Laser Spectroscopy V,* edited by A. R. W. McKellar, T. Oka, and B. P. Stoicheff (Springer, Heidelberg, 1981), p. 260; J. F. Lam, D. G. Steel, and R. A. McFarlane, Phys. Rev. Lett. **49**, 1628 (1982).
[39]J. F. Lam and R. L. Abrams, Phys. Rev. A **26**, 1539 (1982).
[40]D. Bloch and M. Ducloy, J. Phys. B **14**, L471 (1981).
[41]M. Ducloy and D. Bloch, J. Phys. (Paris) **42**, 711 (1981).
[42]D. Bloch, R. K. Raj, and M. Ducloy, Opt. Commun. **37**, 183 (1981).
[43]N. Bloembergen, M. D. Levenson, and M. M. Salour, Phys. Rev. Lett. **32**, 867 (1974).
[44]R. Scholz, J. Mlynek, and W. Lange, Phys. Rev. Lett. **51**, 1761 (1983).
[45]J-L. LeGouet and P. R. Berman, Phys. Rev. A **24**, 1831 (1981).